J Neurophysiol 98: 939–951, 2007.
First published June 20, 2007; doi:10.1152/jn.00423.2007.

Regulation of Burst Dynamics Improves Differential Encoding of Stimulus Frequency by Spike Train Segregation

W. Hamish Mehaffey,[1] Fernando R. Fernandez,[1] Leonard Maler,[2] and Ray W. Turner[1]

[1]*Hotchkiss Brain Institute, University of Calgary, Calgary, Alberta; and* [2]*Cellular and Molecular Medicine, University of Ottawa, Ottawa, Ontario, Canada*

Submitted 13 April 2007; accepted in final form 16 June 2007

Mehaffey WH, Fernandez FR, Maler L, Turner RW. Regulation of burst dynamics improves differential encoding of stimulus frequency by spike train segregation. *J Neurophysiol* 98: 939–951, 2007. First published June 20, 2007; doi:10.1152/jn.00423.2007. Distinguishing between different signals conveyed in a single sensory modality presents a significant problem for sensory processing. The weakly electric fish *Apteronotus leptorhynchus* use electrosensory information to encode both low-frequency signals associated with environmental and prey signals and high-frequency communication signals between conspecifics. We identify a mechanism whereby the $GABA_B$ component of a feedback pathway to the electrosensory lobe is recruited to regulate the intrinsic burst dynamics and coding properties of pyramidal cells for these behaviorally relevant input signals. Through recordings in an in vitro slice preparation and a reduced model of pyramidal cells, we show that recruitment of dendritic $GABA_B$ currents can shift the timing of a backpropagating spike and its influence on an intrinsic burst mechanism. This regulation of burst firing alters the coding properties of pyramidal cells by improving the correlation of burst and tonic spikes with respect to low- or high-frequency components of complex stimuli. $GABA_B$ modulation of spike backpropagation thus improves the segregation of burst and tonic spikes evoked by simulated sensory input, allowing pyramidal cells to parcel the spike train into coding streams for the low- and high-frequency components. As the feedback pathway is predicted to be activated in circumstances where environmental and communication stimuli coexist, these data reveal a novel means by which inhibitory input can regulate spike backpropagation to improve signal segregation.

INTRODUCTION

A common problem faced by sensory systems is how to filter and parse complex stimuli within a single sensory modality to recognize and categorize behaviorally relevant signals from a complex sensory environment. Perhaps the simplest way of accomplishing this is to segregate the response of central neurons to primary afferent input into distinguishable subgroups of spike output. Pyramidal cells in the electrosensory lateral line lobe (ELL) of the weakly electric fish *Apteronotus leptorhynchus* display two modes of firing. One mode consists of a tonic firing regime characterized by regular spiking evoked by weak input currents. As injected current increases, the firing rate increases and eventually the cell progresses into a burst firing mode (Lemon and Turner 2000; Turner et al. 1994). The bursting is characterized by an increasing firing rate that terminates in a high-frequency doublet and postburst pause before the cycle begins again. Both types of discharge can be observed in ELL pyramidal cells recorded in vitro or in vivo, and this dendrite-mediated mechanism has been shown to segregate the spike train such that bursts code preferentially for low-frequency events (Oswald et al. 2004), whereas isolated spikes encode broadband inputs, including high frequencies.

Electric fish receive electrosensory signals with varying frequencies and degrees of spatial correlation (Chacron et al. 2003; Doiron et al. 2003). In general, spatially "local" stimuli are related to prey or environmental objects; movement of the fish past these objects generates low-frequency signals (MacIver et al. 2001). In comparison, spatially correlated "global" inputs are related to important conspecific signals for communication, including "chirps," and beat frequencies generated by the difference in the frequency of electric organ discharge (EOD) between different fish (usually >20 Hz) (E. Fortune, personal communication). These often contain most of their power at high frequencies (Zupanc et al. 2006). One effect of spatially correlated inputs is the recruitment of a direct inhibitory feedback pathway to the ELL (Doiron et al. 2003, 2004) that activates both $GABA_A$ and $GABA_B$ receptors on pyramidal cells (Berman and Maler 1998b). Of course, communication inputs do not preclude the existence of locally occurring prey-like signals, particularly because these fish and related species often forage in small groups (Tan et al. 2005; E. Fortune, personal communication). Distinguishing between these different signals within a single sensory modality is a significant problem, analogous to the "cocktail party effect" discussed in human auditory processing (Cherry 1953; Haykin and Chen 2005), where specific frequencies within an input must be parsed.

Pyramidal cells of the ELL process electrosensory information and are part of a direct closed loop feedback pathway with cells in the more rostral nucleus praeeminentalis (nP). Briefly, pyramidal cells send efferents to the nP bipolar cells, which in turn send inhibitory (GABAergic) fibers back to the ELL through the tractus stratum fibrosum (StF) (Berman and Maler 1999; Maler and Mugnaini 1994) (Fig. 1*A*). This pathway is known to activate both $GABA_A$ and $GABA_B$ receptor-mediated inhibitory postsynaptic potentials (IPSPs) through Cl^- and K^+ conductances in pyramidal cells, respectively (Berman and Maler 1998b). The observed currents arise from synaptic contacts onto the somata and proximal apical dendrites of both types of ELL pyramidal cells, the basilar and nonbasilar pyramidal cells (Maler and Mugnaini 1994) (Fig. 1*A*). The fast $GABA_A$ conductance has been shown to induce a gamma

Address for reprint requests and other correspondence: R. W. Turner, Hotchkiss Brain Institute, University of Calgary, 3330 Hospital Dr. N.W., Calgary, Alberta T2N 4N1, Canada (E-mail: rwturner@ucalgary.ca).

The costs of publication of this article were defrayed in part by the payment of page charges. The article must therefore be hereby marked "*advertisement*" in accordance with 18 U.S.C. Section 1734 solely to indicate this fact.

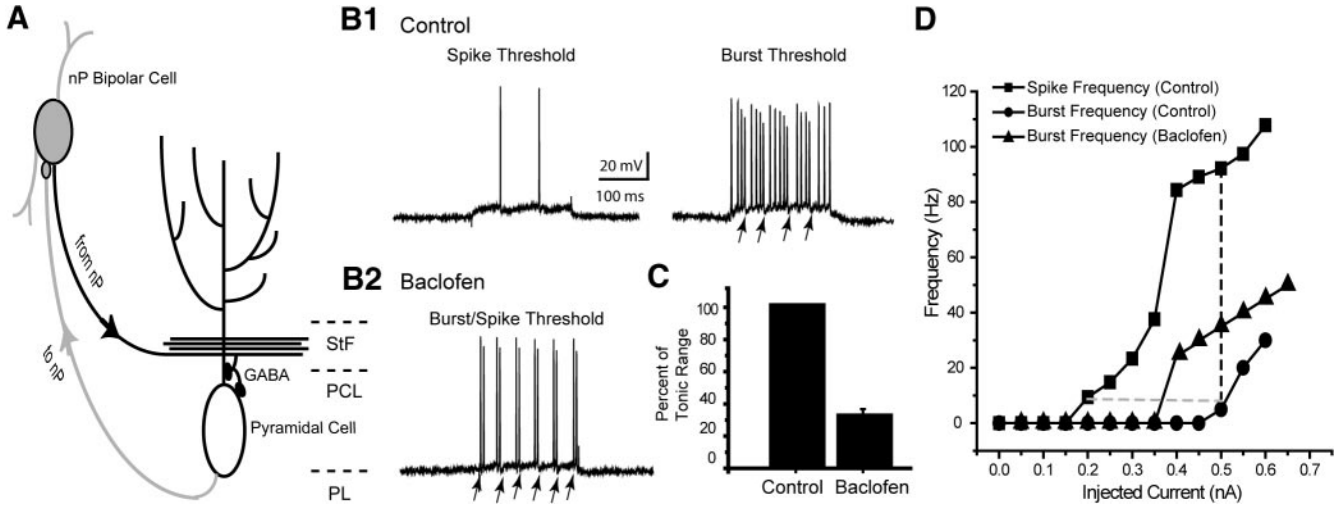

FIG. 1. A direct inhibitory feedback pathway can regulate bursting. *A*: schematic of direct feedback pathway to the electrosensory lateral line lobe (ELL). Pyramidal cell axons project to nucleus praeeminentalis (nP) bipolar cells, which in turn synapse on the pyramidal cell near the soma and along the most proximal apical dendritic region, activating both $GABA_A$ and $GABA_B$ receptor subtypes. *B*: pyramidal cells fire tonically in response to current injection (*B1, left*, 0.2 nA). When the injected current surpasses a 2nd threshold value the cell responds with patterned bursting [*B1, right*, 0.5 nA; arrows, burst afterhyperpolarizations (AHPs)]. Baclofen application to the soma/proximal dendritic region activates $GABA_B$ receptors and the pyramidal cell now responds with spike doublets immediately after crossing spike threshold with no initial tonic firing (*B2,* 0.4 nA). *C*: baclofen leads to a compression of the tonic range of firing as indicated by a significant decrease in the range of current injections between spike threshold and bursting. *D*: plots of the F-I relationship for tonic and burst discharge in a representative cell before and after focal pressure application of baclofen. Dashed lines indicate burst threshold (black), and the tonic firing range (gray) in control conditions.

frequency oscillation in pyramidal cells due to a negative feedback that is recruited when the fish is exposed to electric fields with a spatial configuration similar to electrocommunication signals (Doiron et al. 2003, 2004; Lindner et al. 2005). The oscillation evoked by this input is on the order of 30–50 Hz, and the $GABA_B$ currents recorded in pyramidal cells have a duration of ~500 ms (Berman and Maler 1998b), far too slow to be involved in the genesis of this oscillation. The role of the slow $GABA_B$ component of this feedback pathway has thus not yet been identified.

We have shown previously that the burst mode of firing is caused by an interplay between somatic and dendritic spikes that involves a progressive shift in their temporal separation during repetitive discharge (Fernandez et al. 2005b). We now show that the latency between somatic and dendritic spikes and the related burst discharge can be regulated by dendritic $GABA_B$ inhibition from the descending feedback pathway. This regulation of the burst dynamics leads to an improved segregation of burst and isolated spike coding for low- and high-frequency input, respectively, a process that may regulate signal processing in vivo.

METHODS

Preparation of slices

Weakly electric Brown Ghost knife fish (*A. leptorhynchus*) were obtained from local importers and maintained at 26–28°C in fresh water aquaria in accordance with protocols approved by the University of Calgary Animal Care Committee. All chemicals were obtained from SIGMA (St. Louis, MO) unless otherwise noted. In all cases, recordings were obtained from separate pyramidal cell somata or apical dendrites in in vitro slices. Animals were anesthetized in 0.05% phenoxy-ethanol, and ELL tissue slices of 300- to 400-μm thickness were prepared as previously described (Turner et al. 1994). Slices were maintained by constant perfusion of artificial cerebrospinal fluid (ACSF, 1–2 ml/min) and superfusion of humidified 95% O_2-5% CO_2 gas. ACSF contained (in mM) 124 NaCl, 3 KCl, 25 $NaHCO_3$, 1.0 $CaCl_2$, 1.5 $MgSO_4$, and 25 D-glucose, pH 7.4. Pharmacological agents were ejected locally from a pressure micropipette containing HEPES-buffered ACSF (in mM) 148 NaCl, 3.25 KCl, 1.5 $CaCl_2$, 1.5 $MgCl_2$, 10 HEPES, and 25 D-glucose, pH 7.4.

Stimulation and recording procedures

Glass microelectrodes were backfilled with 2 M KAc (pH 7.4; 90–120 MΩ resistance) and in some recordings, contained 2% Neurobiotin (Vector Labs). Separate recordings were made from dendritic or somatic compartments of ELL pyramidal cells (n = 56) in the two largest ELL segments receiving primary afferent input from P-units (centrolateral and centromedial segments) (Maler et al. 1991). Somatic recordings were made from the pyramidal cell layer and dendritic recordings at the boundary of an easily recognized feedback fiber tract, the stratum fibrosum (StF), and molecular layer containing the apical dendrites of pyramidal cells (Turner et al. 1994). When neurons had been filled with Neurobiotin, the slices were fixed in 4% paraformaldehyde in phosphate-buffered saline and subsequently reacted with streptavidin-conjugated Cy3 in 1.0% Triton-X 100 and 2% DMSO for 48 h for visualization on an Olympus FV300 BX50 confocal microscope. We were therefore able to classify pyramidal cells as basilar (E cell) or nonbasilar (I cell) types. Cell fills were successful in ~55% of cases, giving a total number of 13 nonbasilar cells and 16 basilar pyramidal cells.

Recordings were digitized using a NI PCI-6030E DAQ board (National Instruments, Austin TX). Intracellular stimuli were delivered, and data were recorded in custom software using the Matlab data-acquisition toolbox (Mathworks, Natick MA). Dendritic and somatic recordings were distinguished by the placement of the electrode and from the spike waveform [dendritic spikes in the ELL display a minimal afterhyperpolarization (AHP) and a wider half-width than somatic spikes (Turner et al. 1994)]. Antidromic activation was accomplished with stimulation of the plexiform layer (PL, Fig. 1*A*) using a bipolar tungsten electrode and a fiber pathway exclusively containing pyramidal cell axons that allows specific activation of pyramidal cells (Turner et al. 1994). For dendritic recordings, the

electrode was placed in or slightly above the StF, a ~50-μm-wide fiber tract immediately dorsal to the pyramidal cell layer (PCL, Fig. 1*A*). We therefore believe our dendritic recordings to be within ~100 μM of the soma, although exact distances cannot be precisely known for each recording. Stimulation of the inhibitory component of the StF feedback pathway was accomplished by placing the stimulating electrode at its ventral edge in the presence of 6,7-dinitroquinoxaline-2,3-dione (DNQX), and D (−)-2-amino-5-phosphonopentanoic acid (AP-5) to block excitatory neurotransmission, as previously reported (Berman and Maler 1998a).

Random amplitude modulations (RAMs) consisted of white noise low-pass filtered to 0–60 Hz. As sensory input in this frequency range is well tracked by the membrane potential of pyramidal cells (Chacron et al. 2003; Middleton et al. 2006), these intracellular current injections serve as good mimics of afferent input associated with natural electrosensory signals. RAMs were given near threshold for firing of the cell, and the SD of the waveform was adjusted to give firing rates of 10–25 Hz, which is typical of these cells in vivo (Bastian 1999). Assessments of rheobase for tonic and burst spiking were assessed through a series of 250-ms step until burst threshold was reached ($\leq$1 nA), with 2 s between pulses. Baclofen has previously been shown to activate $GABA_B$ receptors in this preparation and was focally ejected (100 μM) into the PCL using electrodes of 1- to 2-μm tip diameter and 7–15 psi pressure ejection as previously described (Berman and Maler 1998b,c; Turner et al. 1994). A visual estimate of the radius of drug application was initially obtained in dendritic regions under transillumination. Previous studies have estimated a ~10 times dilution factor to obtain effects consistent with bath application (Turner et al. 1991, 1994). Pharmacological agents were dissolved in HEPES-buffered ACSF.

Data analysis

All electrophysiological data were analyzed in Matlab R2006a (Mathworks). Spike threshold was obtained from the first derivative of the voltage waveform. Data were plotted in Origin (OriginLab, Northhampton MA).

Spike trains were partitioned into bursts and isolated spikes using an interspike interval (ISI) histogram method and ISI discrimination criterion of 8 ms in agreement with previous work that established that these ISIs are associated with the conditional backpropagation of dendritic spikes that characterize bursting (Lemon and Turner 2000). This is consistent with previous studies examining in vitro time-varying inputs as burst ISIs can be readily defined using this value given the consistency of burst output between cells in vitro (Oswald et al. 2004). Bursts and isolated spike trains were digitized into binary trains and their mean subtracted (Rieke 1997). Coherence estimates between the digitized spike trains and the original RAM stimulus were calculated as

$$C(f) = \frac{P_s(f)^2}{P_{ss}(f)P_{rr}(f)}$$

where P_{ss} and P_{rr} denote the power spectrum of the stimulus and the response, and P_{sr} denotes the cross-spectrum between the stimulus and response (e.g., the spike train) and f is frequency measured in hertz. Statistical significance was determined using paired t-test unless otherwise noted and expressed as means ± SE. Statistical significance for ANOVA was determined using Tukey's HSD.

Simulations

Simulations were constructed in MatLab 7 using a fourth-order Runge-Kutta algorithm with a time step (dt) of 0.005 ms. All bifurcation analyses were done using the XPP-AUTO package (Doedel 1981; Ermentrout 2002). Our model consisted of a reduction of an ELL pyramidal cell to two compartments (soma and dendrite) that has previously been used to describe bursting in this system (Fernandez et al. 2005b). Our model was described by the following equations

$$m_{s\infty} = \frac{1}{1 + e^{(-(V-40)/3)}}, \quad (1)$$

somatic Na^+ activation

$$\frac{dh_r}{dt} = \frac{-h_s + h_{s\infty}(V)}{\tau_{hs}(V)}, \quad (2)$$

somatic Na^+ inactivation

$$h_{s\infty} = \frac{1}{1 + e^{((V+40)/3)}}, \quad (3)$$

somatic Na^+ steady-state inactivation and K^+ activation

$$\frac{dm_d}{dt} = \frac{-m_d + m_{d\infty}(V)}{\tau_{m_d}(V)}, \quad (4)$$

dendritic Na^+ activation

$$m_{d\infty} = \frac{1}{1 + e^{(-(V+46.7)/5.7)}}, \quad (5)$$

dendritic steady-state Na^+ activation

$$\frac{dh_d}{dt} = \frac{-h_d + h_{d\infty}(V)}{\tau_{h,d}(V)}, \quad (6)$$

dendritic Na^+ inactivation

$$h_{d\infty} = \frac{1}{1 + e^{((V+55)/3)}}, \quad (7)$$

dendritic steady-state Na^+ inactivation

$$\frac{dn_d}{dt} = \frac{-n_d + n_{d\infty}(V)}{\tau_{n_d}(V)}, \quad (8)$$

dendritic K^+ activation

$$n_{d\infty} = \frac{1}{1 + e^{(-(V+12.5)/8.75)}}, \quad (9)$$

dendritic steady-state K^+ activation.

All time constants in the model were voltage-dependent and described by a Lorentzian function as used in a previous study (Fernandez et al. 2005a)

$$\tau(V) = y_0 + \frac{2Aw}{4\pi(V - V_c)^2 + w^2} \quad (10)$$

for h_s: $V_c = -64$, $w = 28$, $A = 232$, $y_0 = 0$;
for m_d: $V_c = -45.7$, $w = 26$, $A = 7.4$, $y_0 = 0$;
for h_d: $V_c = -60$, $w = 43$, $A = 301.6$, $y_0 = 0$;
for n_d: $V_c = -40$, $w = 30$, $A = 70$, $y_0 = 0.4$.

Voltage in the somatic (V_s) and dendritic (V_d) compartments was integrated according to

$$C_s\frac{dV_s}{dt} = \frac{(V_d - V_s)}{\kappa R} + I_E - g_{Nas}m_{s\infty}{}^3h_s(V_s - E_{Na^+}) - g_{Ks}(1 - h_s)^1(V_s - E_{K^+}) - g_{sGABAx}(V_s - E_{K^+}) - g_{leaks}(V_s - E) \quad (11)$$

$$C_d\frac{V_d}{dt} = \frac{(V_s - V_d)}{(1 - \kappa)R} - g_{Nad}m_d{}^3h_d(V_d - E_{Na^-}) - g_{Kd}n_d{}^4(V_d - E_{K^-}) - g_{dGABAx}(V_d - E_{rev,syn}) - g_{leakd}(V_d - E_{leak}) \quad (12)$$

Constants in the somatic and dendritic compartments consisted of the following: $C_s = 1.2$ μF/cm^2, $C_d = 3.5$ μF/cm^2, $R = 2/3$ kΩ/cm^2, κ =

0.35, E_{Na^+} = 40 mV, E_{K^+} = −88.5 mV, E_{leak} = −72 mV, g_{Nas} = 60 mS/cm^2, g_{Ks} = 12 mS/cm^2, g_{leaks} = 0.18 mS/cm^2, g_{Nad} = 20 mS/cm^2, g_{Kd} = 8 mS/cm^2, g_{leakd} = 0.18 mS/cm^2, g_{sGABAb} = 0 mS/cm^2, g_{dGABAb} = 0 mS/cm^2 unless otherwise noted. The GABA-like conductances in the soma and dendrite are denoted as g_{sGABAx} and g_{dGABAx}, respectively, with the associated reversals of −70 mV for $GABA_A$ and −88.5 mV for $GABA_B$ (Berman and Maler 1998a–c). The cell was driven with an external current source (I_E).

The parameter κ denotes the relative contribution of one compartment to the other with a κ value of 0.35 signifying that the dendritic current influence on the soma is greater than the somatic current influence on the dendrite. The R parameter denotes the resistance between the two compartments. The κ and R values are similar to those of previous modeling studies using this approach (Doiron et al. 2002; Mainen and Sejnowski 1996; Pinsky and Rinzel 1994; Wang 1999).

RESULTS

$GABA_B$ receptor activation alters burst dynamics

When stimulated with steps of intracellular current injection, ELL pyramidal cells generally begin firing tonically and with increasing current, shift into a burst firing mode (Fig. 1*B*). Bursting is characterized by a progressive decrease in the ISI, terminating in a fast pair of spikes ("doublet" of 3–10 ms ISI) followed by a burst AHP (bAHP) (Lemon and Turner 2000). This resets the burst cycle, causing a brief pause before the cycle begins again (Fig. 1*B1,* arrows). The range of current injections between spike threshold and bursting is defined as the tonic range of firing (see Fig. 1*D*, gray dashed line). To examine the effects of $GABA_B$ activation, we applied baclofen (100 μM) as a selective $GABA_B$ agonist to the ELL PCL through focal pressure ejection from a small-tipped pipette. Note that because GABAergic afferent axons from nP bipolar cells travel along the ventral StF, we could not use the StF as a barrier to segregate somatic and dendritic effects of ejected drugs as in previous studies (Mehaffey et al. 2005; Noonan et al. 2003; Turner et al. 1994). Therefore the possible locus for our observed baclofen effects include the activation of receptors at pyramidal cell somata and the most proximal regions of the apical and basilar dendrites (Maler and Mugnaini 1994).

Pressure ejections of baclofen in the PCL rapidly evoked a decrease if not a complete elimination of the tonic firing range of pyramidal cells. Rather cells could repetitively fire spike doublets from the onset of firing instead of exhibiting the normal range of tonic firing and then bursting (Fig. 1*B2*). Figure 1*D* shows a representative FI plot displaying the full range of firing behaviors before and after baclofen ejections. As injection current increased in control conditions, pyramidal cells fired faster and eventually began to burst. After baclofen ejection, the tonic range of firing was abolished, and cells began to burst immediately on crossing rheobase, effectively lowering the threshold for bursting (Fig. 1, *B–D*). Although not all cells showed a direct transition to bursting (n = 4 of 11), all pyramidal cells examined displayed a compression of the tonic firing regime, with an average 69 ± 5% decrease in the tonic range of firing ($P < 0.01$; n = 11; Fig. 1*C*). Neurobiotin labeling showed that these effects occurred in both basilar and nonbasilar classes of pyramidal cells (n = 4 nonbasilar, n = 3 basilar).

Further, on activation of inhibitory receptors, there was a corresponding increase in rheobase of 120 ± 40 pA ($P <$ 0.05). Although this is consistent with the predicted effects of inhibition, a compression of the tonic firing regime is distinct from the effects of inhibition in other cells. Most often, inhibition leads to a subtractive change in rheobase but does not alter the firing dynamics of the cell (e.g., Mehaffey et al. 2005; Ulrich 2003). In this case, inhibition was able to qualitatively alter the firing behavior of ELL pyramidal cells.

$GABA_B$ pathways in the ELL

The $GABA_B$ receptors affected by baclofen ejection could correspond to those normally activated by the direct feedback pathway through the StF that synapses on the soma and proximal apical dendrites of pyramidal cells or by inputs from ovoid cells which synapse on the basal dendrites of basilar pyramidal cells (Bastian et al. 1993; Berman and Maler 1999; Maler and Mugnaini 1994). As the basal dendrite does not contribute to the burst mechanism in pyramidal cells (Turner et al. 1994), we can reduce the possible loci of $GABA_B$ inhibition that promotes burst discharge in basilar pyramidal cells to either the soma or the proximal apical dendrite. Nonbasilar pyramidal cells exclusively receive $GABA_B$ mediated inhibition from nP bipolar cells (Berman and Maler 1998c). Because we observe compression of the tonic firing regime in both basilar and nonbasilar pyramidal cells, we suggest that the nP bipolar cell direct feedback pathway is the source of input to activate the $GABA_B$ currents mediating our results.

Stimulation of the StF can regulate burst threshold

To more rigorously test whether the StF is the source of the inhibition that regulates bursting, we compared the firing of pyramidal cells without, or immediately after, activation of the StF fiber bundle (10× stimulation at 100 Hz). Stimulation of this pathway in the presence of DNQX generated an isolated slow, long-lasting IPSP of ≤500 ms (Fig. 2*A*). The apparent absence of fast IPSPs is likely due to the cell being held near the reversal potential for chloride (approximately −70 mV) (Berman and Maler 1998a) during stimulation. This slow IPSP has been previously shown to be $GABA_B$ receptor mediated and is sensitive to common $GABA_B$ antagonists (Berman and Maler 1998b). By pairing StF stimulation with a 200-ms depolarizing current pulse timed such that it overlapped the peak of the IPSP (after 50- to 100-ms delay after the end of the stimulus train), we were able to compare the firing frequency and burst thresholds of pyramidal cells with and without activation of the StF $GABA_B$ pathway (Fig. 2*B*). As found for baclofen ejections, stimulating the StF inhibitory pathway significantly compressed the tonic firing regime and increased the rate of burst firing (Fig. 2*C*). The tonic firing range was compressed to 62 ± 8% of the control range ($P < 0.01$, n = 5). Although no cells transitioned directly to bursting, this is consistent with the expected incomplete recruitment of $GABA_B$ receptors during 100-Hz stimulation (Berman and Maler 1998b). Most importantly, these results suggest that direct StF stimulation of inhibitory inputs produces similar results to that evoked by focal pressure ejection of baclofen, confirming that the direct feedback pathway is sufficient to activate the necessary mechanisms to regulate burst output via $GABA_B$ receptors in the somatic and proximal dendritic region of pyramidal cells.

Two-parameter bifurcation suggests a dendritic locus for $GABA_B$-mediated burst regulation

To analyze possible mechanisms for GABAergic compression of the tonic range of firing, we used a reduced two-compartment model of the ELL pyramidal cell that has been shown to accurately reproduce the dynamics of pyramidal cell bursts (Fernandez et al. 2005b). This model included primarily currents underlying spike discharge (Na^+, K^+) in both the somatic and apical dendritic compartments that were coupled through a resistance (Fig. 3*A*; see METHODS). We began by performing a two-parameter bifurcation analysis on the model using XPPAUT (Doedel 1981; Ermentrout 2002). Briefly, the two-parameter bifurcation allows us to track either the saddle node of fixed points (SNFP) or the saddle node of limit cycles (SNLC) bifurcation as a function of two parameters in the model (1 of the 2 possible GABA conductances g_{GABAB}, g_{GABAA} and the driving current I). These bifurcations correspond to the transition from quiescence to tonic spiking and from tonic spiking to bursting, respectively (Fernandez et al. 2005b). We modeled $GABA_B$ receptor activation as a tonic K^+ conductance in either the dendritic compartment (g_{dGABAB}) or somatic compartment (g_{sGABAB}) and examined the effects of depolarizing the model through current injection (Fig. 3*A*).

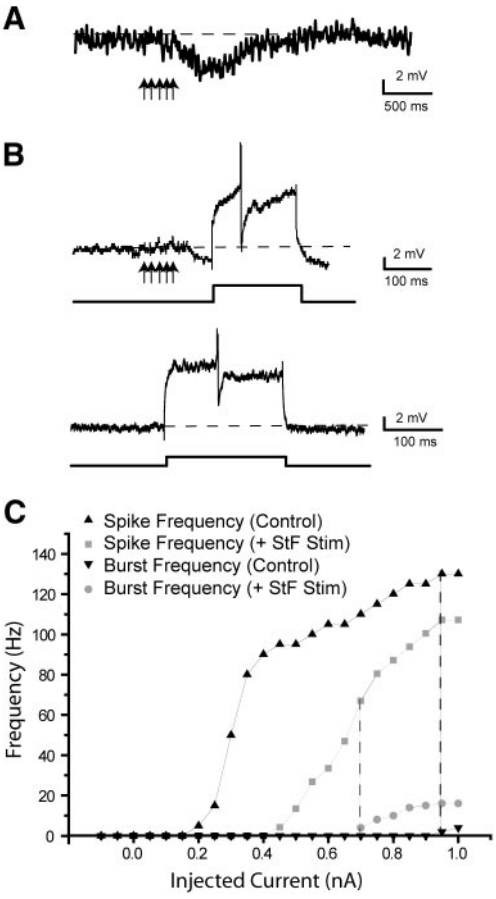

FIG. 2. Stimulation of the inhibitory component of the tractus stratum fibrosum (StF) is capable of regulating bursting. *A*: stimulation of the nP bipolar cell feedback pathway in the StF (10 stimuli, 100 Hz) generates a slow inhibitory postsynaptic potential (IPSP). *B*: pairing activation of the slow IPSP with a pulse of intracellular current (200 ms) allows the F-I curve to be assessed during synaptic activation of the $GABA_B$ receptors. ↑, StF stimuli after which a clear hyperpolarization can be observed (- - -). *Bottom*: control record without synaptic stimulation where no hyperpolarization is evident (- - -). Stimulus artifacts have been truncated. *C*: stimulation of the StF pathway regulates bursting, causing a compression of the tonic firing region. Dashed lines indicate threshold for bursting, the point where the cell ceases tonic firing and begins to burst. Note that StF stimulation compresses the tonic firing range and lowers rheobase for burst firing.

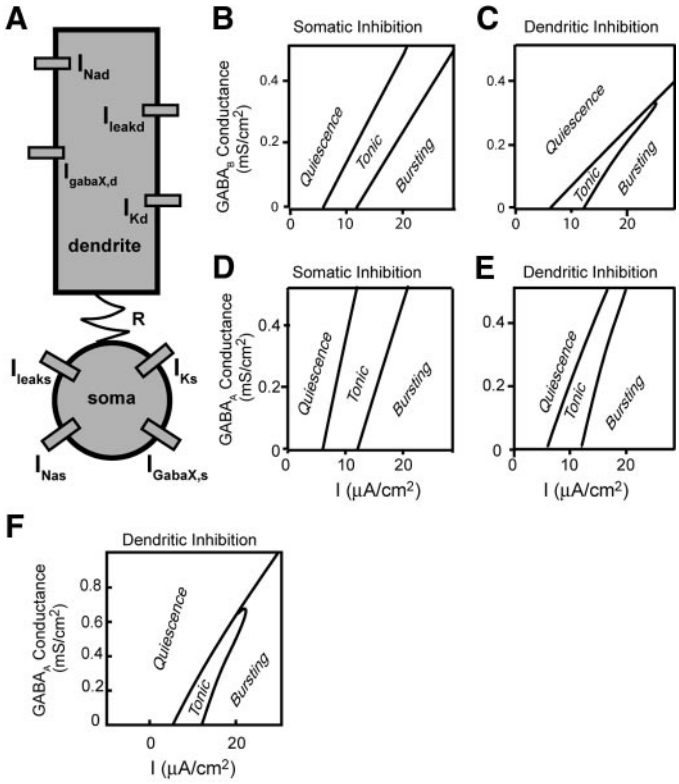

FIG. 3. Two parameter bifurcation analysis of a reduced compartmental model using driving current (I) and GABA conductances as test parameters. *A*: schematic diagram listing the currents involved in the 2-compartment model. R represents a coupling coefficient between somatic and dendritic compartments. *B* and *C*: addition of $GABA_B$ conductance ($E_{rev} = -88.5$ mV) to the soma (*B*) raises tonic firing and burst threshold but fails to compress the tonic range of firing. However, addition of this conductance to the dendrites (*C*) leads to a significant compression of the tonic range of firing and promotes an earlier shift to bursting. *D* and *E*: when a conductance reversing at −70 mV (E_{cl}, $GABA_A$-like) is added to the soma, no compression of the tonic region is noticeable. A minor compression can be seen after addition of large amounts of the $GABA_A$ conductance to the dendritic compartment. *F*: expanded view of the 2-parameter bifurcation for the $GABA_A$ conductance showing that large amounts of inhibition are able to compress the tonic firing regime but require a larger conductance than that for the $GABA_B$ conductance. Note in particular, that the tonic firing regime collapses much more suddenly in the $GABA_A$ condition as opposed to the graded compression observable in the $GABA_B$ condition (*C*).

When we performed a two-parameter bifurcation analysis using $GABA_B$ conductances placed somatically, we observed no change in the distance between the fold points associated with firing threshold and burst threshold—both points were right shifted by an equal amount (Fig. 3*B*). After $GABA_B$ conductances were placed in the dendrites, we observed a compression of the tonic firing regime that increased with the level of dendritic $GABA_B$ conductance (g_{dGABAB}; Fig. 3*C*). This compression continued until the tonic regime was completely extinguished at $g_{dGABAB} \approx 0.4$ mS/cm^2, defining the region of parameter space where the tonic firing regime was abolished. The transition to burst threshold was still through a saddle node of fixed points, so the cell still conformed to type

I excitability (e.g., the model remains capable of an infinitely slow approach to threshold) (Rinzel and Ermentrout 1998). However, now each time that the cell crossed threshold, two spikes (the "doublet") were created rather than one.

We note that our reduced model produced a large increase in firing threshold compared with our results from in vitro recordings on activation of dendritic $GABA_B$ conductance. This discrepancy is due to the κ term in the model, which represents the relatively larger influence of the dendrite as compared with the soma. Although necessary to allow for the reduction of the entire dendrite to a single compartment, this leads to an overestimate of the effect of inhibitory dendritic conductances on the firing threshold of the cell. This reduction is valuable, however, in that it allows us to perform the types of analysis discussed in the preceding text, in particular the two-parameter bifurcation analysis, and has generated significant insights in both our system (Doiron et al. 2002; Fernandez et al. 2005b), and others (Pinsky and Rinzel 1994; Wang 1999). It has been shown previously that in spatially extensive models and in real cells, dendritic inhibition in fact has less of an effect on spike threshold (Mehaffey et al. 2005), consistent with our in vitro results. Thus despite the overestimate of the rheobase shifts during dendritic inhibition, the model was able to reproduce the key salient feature (a compression of the tonic firing regime). Further, as we show in the following text, the model also correctly predicts many features of dendritic inhibition on cell dynamics and coding properties.

Pyramidal cells also receive Cl^--mediated inhibition through $GABA_A$ conductances from a wide variety of feedforward and feedback pathways that contact both the somata and dendrites (Berman and Maler 1998a, 1999). We therefore again carried out a two-parameter bifurcation but instead using an inhibitory conductance meant to replicate Cl^--mediated $GABA_A$ inputs. When the $GABA_A$ conductance was distributed somatically (g_{sGABAA}), no compression of the tonic firing regime was obtained (Fig. 3*D*), whereas a dendritic distribution (g_{dGABAA}) led to only a slight compression of the tonic firing regime within an equivalent range (Fig. 3*E*). Dendritic $GABA_A$ was eventually able to abolish the tonic firing regime, but only at much larger conductances (Fig. 3*F*). To examine the possibility of $GABA_A$ modulation of pyramidal cell bursting, we ejected muscimol (100 μM), a selective $GABA_A$ agonist, to the PCL. As predicted by the model, muscimol failed to compress the firing regime of pyramidal cells significantly ($9 \pm 27\%$ of control, $P > 0.05$, $n = 13$; data not shown). Interestingly, the model predicts a more abrupt collapse of the tonic firing regime with $GABA_A$ as compared with the more graded response observed with $GABA_B$ inhibition. This may partially account for the lack of any observed effects during application of $GABA_A$ antagonists. Our data and model therefore show that within the physiological conductance range, hyperpolarization caused by $GABA_A$ inhibition at either proximal apical dendritic or somatic sites is not capable of compressing the tonic firing range.

Biophysical interpretation of burst regulation

The effects of $GABA_B$ activation on actual spike output is summarized in Fig. 4. As documented in Fig. 3, *B* and *C*, adding a somatic $GABA_B$-like inhibitory conductance (g_{sGABAB}) to the model was ineffective at producing a shift to

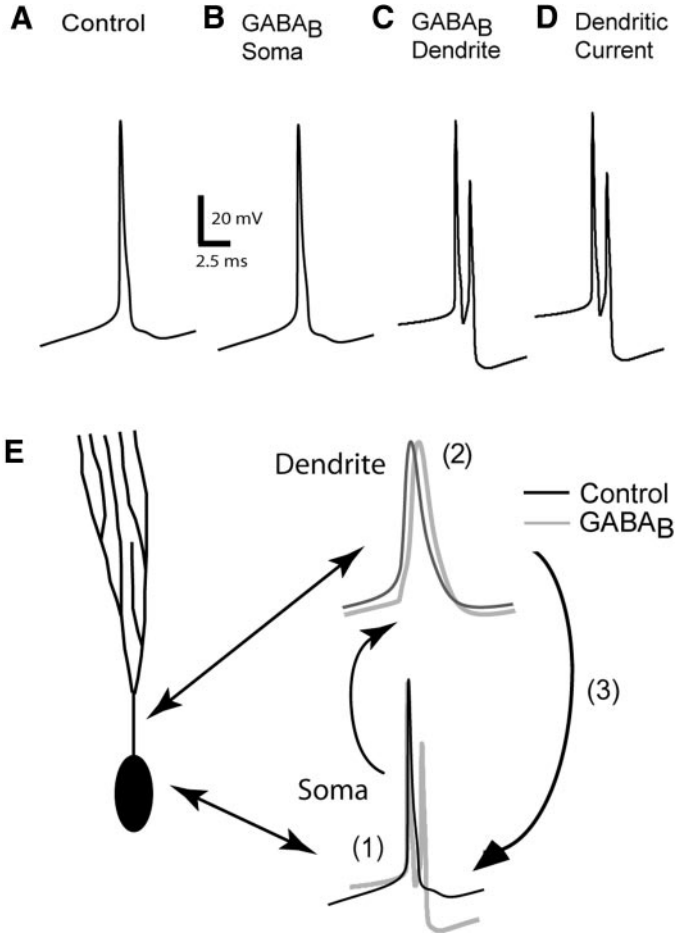

FIG. 4. A 2-compartment model suggests a mechanism for compression of the tonic firing range by $GABA_B$ receptor activation. *A*: somatic spike in the model under control conditions ($g_{s,dGABAb} = 0$ mS/cm^2). *B*: when $GABA_B$ currents are added to the soma ($g_{sGABAb} = 0.4$ mS/cm^2), the spiking is unaffected. *C*: when identical currents are added to the dendritic compartment ($g_{dGABAb} = 0.4$ mS/cm^2), the cell develops doublet spikes, replicating the results seen after baclofen application to pyramidal cells in vitro. *D*: these dynamics can be replicated in the model by applying direct hyperpolarizing current injection to the dendritic compartment, suggesting that dendritic hyperpolarization is sufficient to regulate bursting. *E*: schematic diagram of a pyramidal cell and superimposed records of somatic and dendritic activity in the model before and after a change in firing properties. In the model, either dendritic hyperpolarization or addition of the $GABA_B$ current (shown here) delays the dendritic spike (2) relative to the somatic spike (1). This shifts the dendro-somatic feedback underlying a depolarizing afterpotential (DAP, 3) further outside the somatic refractory period, allowing the generation of a 2nd somatic spike that signifies the transition to burst output.

burst firing (Fig. 4, *A* and *B*). By comparison, dendritic $GABA_B$-like inhibition (g_{dGABAB}) replicated the decrease in tonic range of firing and the transition to a pure doublet mode of firing observed in our experimental results (Fig. 4*C*). Our model thus suggests that the $GABA_B$-induced compression of the tonic firing range seen experimentally is due to inhibition of the apical dendrite. We therefore suggest that the compression of the tonic firing regime recorded in vitro requires activation of dendritic $GABA_B$ receptors from the nP bipolar cell feedback pathway.

The change in the dynamics of pyramidal cell output invoked by dendritic $GABA_B$ conductances can be understood if we consider the normal dynamics of bursting in this system. Normally, spikes in ELL pyramidal cells are initiated near or at

the soma and backpropagate along the dendrite. The dendritic spike is broader and occurs with a delay relative to the somatic spike. The resulting voltage discrepancy between the somatic and dendritic compartments causes a dendro-somatic current flow (Fig. 4*E*), giving rise to a depolarizing afterpotential (DAP) at the soma. In the normal dynamics, burst doublets result when repetitive firing promotes a gradual shift in the dendritic spike rate of rise due to sodium channel inactivation (Fernandez et al. 2005a). The progressive delay in the peak of the dendritic spike acts to delay dendro-somatic current flow sufficiently such that the DAP falls outside of the somatic refractory period, causing a second somatic spike (Fig. 4*E*). The ISI of the somatic spike doublet, however, falls within the refractory period of apical dendrites, resulting in the conditional backpropagation that terminates a burst.

The effects of dendritic $GABA_B$ receptor activation could result through membrane hyperpolarization or the underlying conductance change. However, the model suggests that a shift to burst output does not require any change in membrane conductance as the transition could be produced by hyperpolarizing dendritic current injection (Fig. 4*D*). In the model, the effects of dendritic hyperpolarization were distinct in that membrane potential shifts lower than −75 mV augmented the transition to burst by imposing an initial delay in the onset of the dendritic spike rather than slowing the rate of rise of the dendritic spike. As a result, the dendritic depolarization extended beyond the somatic refractory period to force a second spike, signifying the transition to burst firing (Fig. 4*E*). In comparison, Cl^--mediated $GABA_A$ conductances in the model with a reversal potential more depolarized than −75 mV do not hyperpolarize the dendrite sufficiently to delay the dendritic spike or invoke a graded compression of the tonic firing regime. The model thus provides a directly testable hypothesis for how the pyramidal cell may change its behavior after activation of GABA conductances. Briefly, hyperpolarizing dendritic inhibition through $GABA_B$ receptor activation should delay the dendritic spike in a voltage-dependent manner.

Dendritic inhibition selectively delays the onset and peak latency of dendritic spikes

To test the preceding hypothesis, we carried out recordings from pyramidal cell proximal dendrites near or within the StF. In control conditions, the dendrite had a mean resting potential of −64.5 ± 1.1 mV ($n = 5$). After application of baclofen, the dendrite hyperpolarized to −81.4 ± 1.8 mV (Fig. 5*A*; $P < 0.05$). This hyperpolarization occurred along with an increase in latency of 0.87 ± 0.14 ms ($P < 0.05$; $n = 4$) between the antidromic stimulus and the peak of the dendritic spike. However, the shift in dendritic spike latency was not accompanied by a decrease in the rate of rise of the evoked spike (2 ± 5.0%; $n = 4$, $P > 0.05$). In comparison, under these circumstances, the soma hyperpolarized by only 4.7 ± 1.5 mV ($n = 11$), consistent with the degree of somatic hyperpolarization ob-

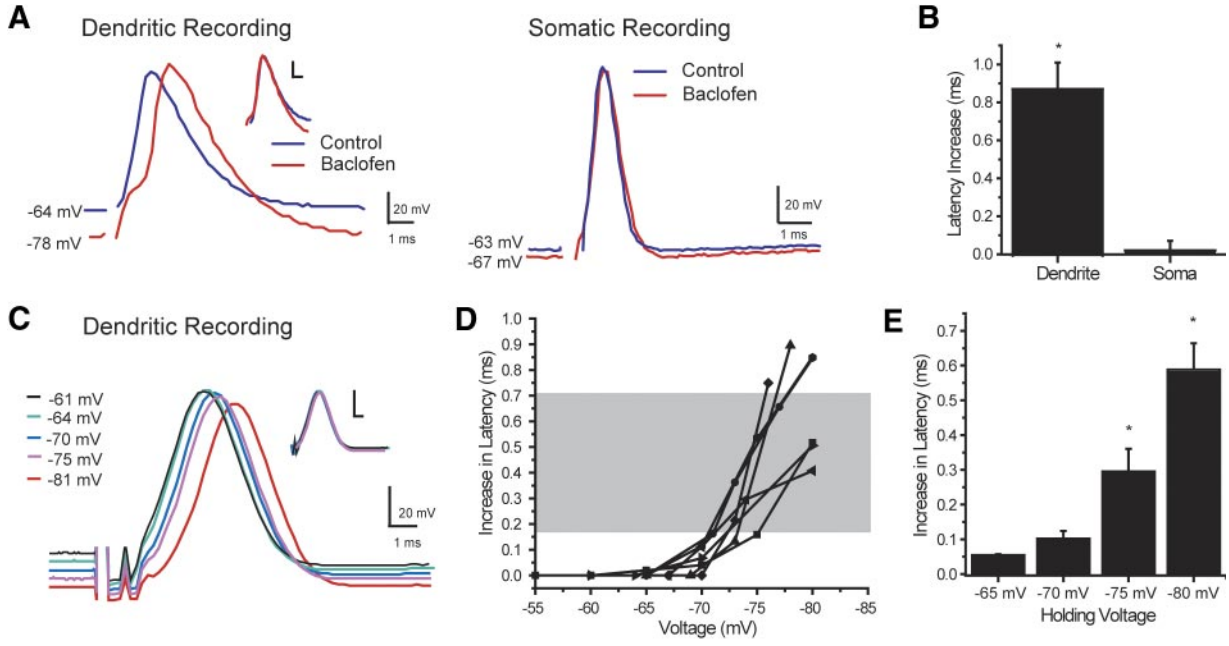

FIG. 5. Hyperpolarization delays the onset and peak of dendritic spikes in pyramidal cells. *A*: superimposed representative recordings of antidromic dendritic or somatic spikes before and after pressure application of baclofen (100 μM) in the pyramidal cell layer (PCL). Baclofen induces a large membrane hyperpolarization at dendritic sites and a pronounced increase in the delay of dendritic spike onset and peak latency with no change in spike rate of rise. By comparison, baclofen has little effect on somatic membrane potential, spike latency or rate of rise. *Inset*: superimposed control and test dendritic spikes aligned for comparison of spike rate of rise. Stimulus artifacts are truncated. *B*: plot of average increase in latency to peak of dendritic or somatic spikes before and after baclofen application, showing that spike latency is selectively increased in the dendrite. *C*: representative example from a proximal dendritic recording of antidromic backpropagating spikes evoked from different levels of membrane potential superimposed for comparison. With increasing amounts of hyperpolarization, the onset and peak of the dendritic spike is increasingly delayed without affecting the rate of rise or repolarization. *Inset*: all records superimposed and aligned to spike peak. *D*: plots of the increase in spike latency observed in all dendritic recordings at varying holding potentials ($n = 11$). The region designated by ▨ corresponds to the range of increases in dendritic spike latency previously observed during burst discharge (Fernandez et al. 2005b), indicating that the shifts in dendritic spike latency during hyperpolarization are representative of those known to occur during repetitive activity. *E*: summary plot of dendritic spike data shown in *D*, indicating that a significant increase in dendritic spike latency occurs at voltages below approximately −72 mV. Data in *E* were binned in 5-mV increments.

served during stimulation of the inhibitory StF feedback pathway (Berman and Maler 1998b). In addition, the somatic antidromic spike did not display a significant change in delay (0.02 ± 0.05 ms of control, $n = 3$, $P > 0.05$) or rate of rise during baclofen application (Fig. 5, *A* and *B*). This confirms that inhibition due to baclofen application is insufficient to delay the somatic spike and yet has a substantial effect on dendritic spike latency.

To determine if these effects on dendritic spike latency were attributable to the baclofen-induced conductance change or membrane hyperpolarization per se, we varied the resting potential of dendritic membrane through DC injections. Cells were held between −55 and −85 mV, and spikes were generated antidromically to measure the delay between the stimulus and evoked spike. Here we found that injecting hyperpolarizing current also increased the peak delay of the antidromic dendritic spike in a voltage-dependent fashion by up to ~1.5 ms. Notably this hyperpolarization did not change the rate of rise of the dendritic spike (4 ± 3% change between the least and most hyperpolarized recordings, Fig. 5*C, insets*, $P > 0.05$). Spike delay was not significantly increased for voltages ranging between −55 and −72 mV ($P > 0.05$, 1-way ANOVA) but showed a significant increase in delay when the resting membrane voltage was held at potentials of −75 mV or lower (0.28 ± 0.06 ms, $P < 0.05$, 1-way ANOVA) and increased further as the voltage approached −85 mV (0.57 ± 0.08 ms, $P < 0.05$, 1-way ANOVA, Tukey's HSD; Fig. 5, *D* and *E*). Importantly, the delays in dendritic spike latency measured for either baclofen application or the more hyperpolarized holding potentials were within the range of those previously measured during repeated high-frequency antidromic stimulation (100 Hz, Fernandez et al. 2005b). The shifts in dendritic spike latency thus fall within the normal range of increased delays that occur during burst discharge (Fig. 5*D*, shaded area, 0.2- to 0.7-ms increase in latency (data from Fernandez et al. 2005b). Sufficient dendritic hyperpolarization (below approximately −72 mV) is thus capable of generating the delays observed during the repetitive firing leading up to bursts and is consistent with the greater activation of $GABA_B$-induced hyperpolarization of dendritic membrane.

Taken together, these results suggest that, as in the model, $GABA_B$ activation in pyramidal cells leads to a hyperpolarization of the dendrite, which in turn selectively delays the peak latency of the dendritic spike. By increasing the soma-dendritic spike delay the backpropagating spike can immediately transition the cell to burst firing through its influence on the somatic DAP.

Compression of the bursting regime alters spike train segregation

After analyzing the mechanism responsible for $GABA_B$ regulation of pyramidal cell bursting, we proceeded to determine the possible effects on information transmission in the ELL. In response to time-varying stimuli, the burst mechanism produces a bimodal ISI distribution that distinguishes bursts and isolated spikes of spike trains both in vivo and in vitro (Gabbiani et al. 1996; Oswald et al. 2004). It has previously been shown that bursts preferentially code for low-frequency (e.g., prey-like and environmental) components of the stimulus, whereas isolated spikes code for both low- and high-frequency signals related to electrocommunication (Oswald et al. 2004). Our finding of a dendritic $GABA_B$ regulation of burst discharge could thus modulate the coding strategies of pyramidal cells.

To test for $GABA_B$ regulation of coding, we placed the model into two conditions based on the response to constant current injections. This consists of a control condition ($g_{dGABAB} = 0.0$ mS/cm^2) and a bursts-only condition ($g_{dGABAB} = 0.4$ mS/cm^2). The model was held near threshold as in previous studies (Oswald et al. 2004) and driven with a frozen noise stimulus. These conditions allowed us to examine the effects of increased bursting on the model's ability to code time-varying inputs. In particular, these effects cannot be explained by the increase in rheobase due to inhibition as the cells were maintained near threshold. Therefore the following results are not due to inhibition causing a failure to respond to weak stimulus components but are due to the change in intrinsic dynamics after dendritic inhibition. As a stimulus, we chose frozen RAMs filtered to contain power between 0 and 60 Hz and compared the stimulus-response coherence with or without the dendritic $GABA_B$ conductance. Figure 6 plots the coherence between the spike train and the RAM with the spike train parsed into bursts and isolated spike components. When inhibition was placed in the dendrites, inducing the bursts-only regime ($g_{dGABAb} = 0.4$ mS/cm^2), we observed a small increase in the burst coherence with high frequencies (defined as 30–50 Hz, Fig. 6*A*). This was paired with a large decrease in the coherence of isolated spikes and low-frequency components of the stimulus (defined as 0–20 Hz, Fig. 6*B*). In comparison, the coherence between isolated spikes and high-frequency components of the stimulus was not decreased.

Thus the nonlinear interaction of dendritic inhibition with the intrinsic dynamics of the two-compartment model is able to significantly affect the coding of inputs. Closer inspection of data records revealed that this occurs because the increased sensitivity of the burst mechanism in the presence of dendritic inhibition prevents small-amplitude, low-frequency inputs from generating isolated spikes, restricting their occurrence to the high-frequency components of the stimulus. Thus isolated spikes are preferentially caused by high-frequency components of the stimulus as the sharp decrease of excitatory input due to fast stimulus downstrokes is able to prevent burst discharge.

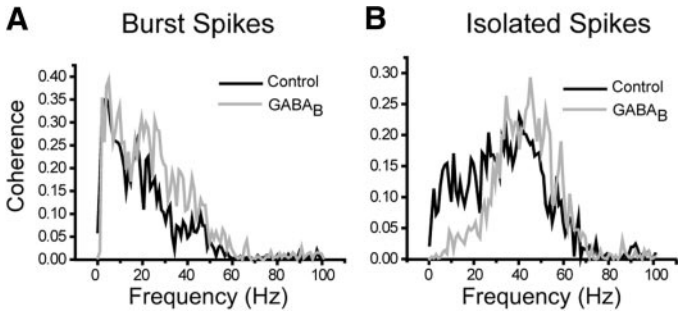

FIG. 6. Compression of the tonic firing region redistributes spike segregation in the model. The model is driven with a frozen white noise current injection at the soma. And the stimulus-response coherence is calculated for burst and tonic spikes. *A*: during dendritic inhibition and compression of the tonic range of firing, the stimulus-response coherence for bursts of spikes is slightly increased (gray trace) relative to control (black trace) and remains preferentially coherent with low-frequency components of the stimulus. *B*: in comparison, coherence between the stimulus and the isolated spikes decreases in the low-frequency regions (gray trace) relative to control (black trace).

This suggests that $GABA_B$ input to the proximal apical dendrites can switch the cell to a mode where the coding of broad-band signals becomes almost completely segregated such that bursts code for low frequencies and isolated spikes code preferentially for high frequencies.

We tested the model's prediction in ELL pyramidal cells in vitro by activating $GABA_B$ receptors with pressure ejection of baclofen while driving the cells from near threshold with an identical frozen RAM stimulus to that used in the model ($n = 7$). As shown previously (Oswald et al. 2004), a pyramidal cell's response to a RAM under control conditions reflects an overall broad-band coherence to the stimulus when the combined output of isolated and burst spikes are considered (Fig. 7, left). The specific responsiveness of isolated or burst spikes can then be parsed out for separate consideration as performed for the model. This analysis shows that the response of isolated spikes in pyramidal cells to the RAM stimulus encompasses a relatively broad band component with a small peak in power at ~40 Hz (Fig. 7, *left*). Burst spikes instead show a preferential coherence to lower frequency components with a peak power ~10 Hz (Fig. 7*A*).

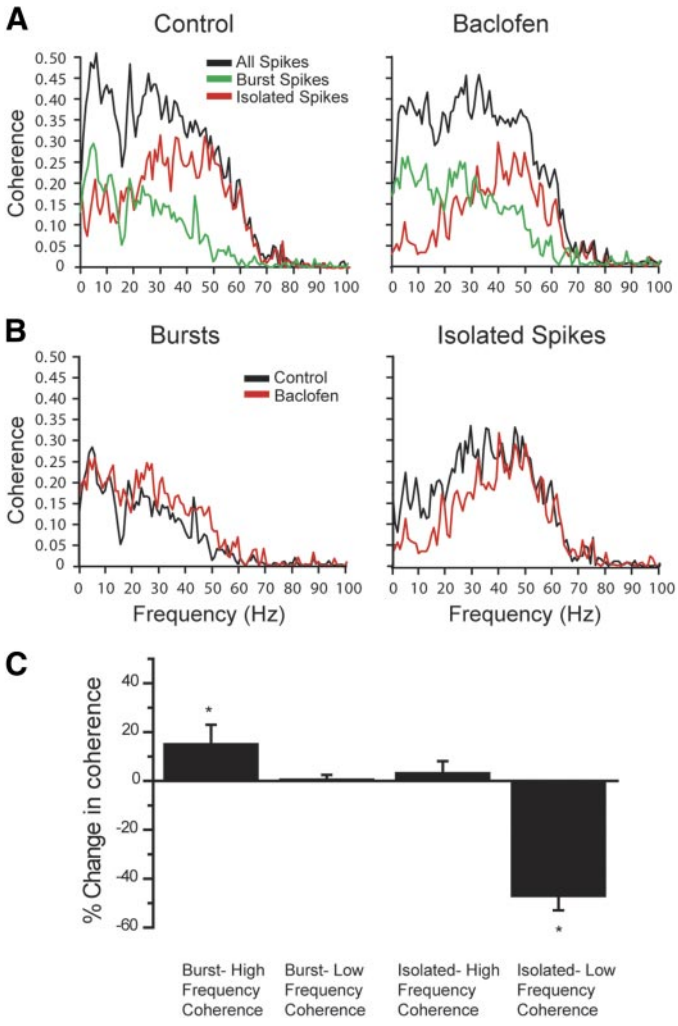

FIG. 7. Experimental confirmation of model predictions. *A*: application of baclofen to a pyramidal cell in vitro causes a shift in firing properties that matches that in the model—the coherence of bursts is slightly increased (green trace) and the low-frequency component of the isolated spike coherence (red trace) is reduced. Note that the overall coherence for all spikes (black trace) is minimally affected. *B*: control coherence (black trace) vs. coherence observed when the tonic firing range is reduced by baclofen (red trace) for burst spikes (*left*) and isolated spikes (*right*) plotted for comparison. *C*: percent changes in the mean coherence for high (30–50 Hz)- and low (0–20 Hz)-frequency stimulus components and bursts or isolated spikes.

After baclofen application had compressed the tonic range of firing, we observed effects similar to those predicted by the model with dendritic inhibition (cf. Figs. 6 and 7*B*). In comparison to control, baclofen application caused a small increase in burst coherence at high frequencies. However, the coherence between isolated spikes and low-frequency inputs was more dramatically reduced (Fig. 7*B*). We quantified this by comparing the mean coherence for 0–20 Hz (low frequency) and for 30–50 Hz (high frequency) before and after application of baclofen. The coherence between bursts and high-frequency events showed a modest but significant increase ($15 \pm 8\%$ from control, $P < 0.05$), whereas coherence between bursts and low-frequency events did not significantly change ($0.5 \pm 2\%$, $P > 0.05$). As predicted by the model, the coherence between isolated spikes and high-frequency events did not change (Fig. 7*B*; $2 \pm 5\%$, $P > 0.05$). Rather, the most significant change was in the coherence between isolated spikes and low-frequency events, which decreased by $47 \pm 6\%$ relative to control values (Fig. 7*B*; $P < 0.05$). We further calculated the burst fraction as the percentage of bursts relative to the total number of spikes. Baclofen induced a significant increase in the burst fraction from 22 ± 4 to $31 \pm 7\%$ of all events ($P < 0.05$). Thus the increase in bursting caused a redistribution of the stimulus-response coherence between bursts and isolated spikes. This allowed a greater segregation of separate components of complex stimuli as summarized in Fig. 7*C*.

DISCUSSION

Distinguishing between different signals imposed simultaneously on a sensory modality is a problem requiring specialized neural systems. In the electric fish, amplitude modulations (AMs) of their electric organ discharge signal are caused both by prey (or inanimate objects) and communication signals from conspecifics. The frequency ranges of AM modulations associated with these signals is very different, however: prey causes low-frequency AMs (<20 Hz), whereas electrocommunication signals can range up to >200 Hz. One mechanism shown to be used by ELL pyramidal cells is to segregate behaviorally relevant frequencies of input by partitioning the spike train into distinct patterns of bursts and isolated spikes (Oswald et al. 2004). Work both in vitro and in vivo has established that bursts code selectively for low frequencies, whereas isolated spikes are broadband and are able to code for the entire frequency range (Doiron et al. 2007; Oswald et al. 2004, 2007). The extensive work completed on the dynamics of spike output in pyramidal cells allowed us to test the specific role of $GABA_B$ receptors activated by an inhibitory feedback pathway on spike firing and coding in pyramidal cells. The present study shows that the dendritic $GABA_B$ receptor component activated by descending feedback can regulate a burst mechanism intrinsic to pyramidal cells by shifting the relative timing of somatic spikes and backpropagating spikes to enhance burst output. In doing so, it induces an improved segregation of the spike train output by allowing isolated spikes to code preferentially for the high-frequency range of input sig-

nals. We propose that the resulting increased segregation of spike firing will improve the ability to detect both prey-like objects (bursts) and communication signals (isolated spikes) when these two signals occur simultaneously. Such segregation of spike trains into distinct components related to different elements of the sensory environment may also be considered as a form of figure-ground discrimination, which can also have a strong temporal component (Fahle 1993). Although most commonly studied in the visual system, the auditory system appears to be capable of regulating neural activity in a similar fashion (Fritz et al. 2007). Such spike train segregation may be helpful in separating relevant environmental cues from a complex background, including communication calls and beat frequencies arising from differences in the EOD frequency between nearby fish.

In the context of figure-background discrimination, the mechanism described here allows specific environmental signals (e.g., prey) to be distinguished from a complex background without necessarily suppressing neural activity that represents this background. It should be noted, however, that the shift in rheobase associated with the inhibition observed here may contribute to such a background suppression. As isolated spikes have been proposed to be sufficient for signal reconstruction, whereas bursts detect low-frequency features, the loss of isolated spikes may decrease the ability to accurately encode low-frequency events. Bursts, however, have been shown to be capable of accurately encoding low-frequency events through their ISIs (Doiron et al. 2007; Oswald et al. 2007). This coding may be improved by more reliable bursting in response to low-frequency stimuli. Understanding the final impact of shifts in spike segregation will require a greater understanding of the decoding of pyramidal cell spike trains by target midbrain neurons.

A schematic of our suggested model of the function of the $GABA_B$ feedback pathway is shown in Fig. 8. When a conspecific is present (Fig. 8*A*), the activation of ELL pyramidal cells by the sensory stimulus recruits the direct feedback pathway from nP bipolar cells (Fig. 8*B*). This causes both a ~30- to 50-Hz $GABA_A$ mediated oscillation (Doiron et al. 2003) and a more tonic inhibition by the slower $GABA_B$ receptors (Fig. 8*C*). The longer-lasting $GABA_B$-mediated hyperpolarization delays the pyramidal cell backpropagating dendritic spike (Fig. 8*D*) and thereby compresses the tonic firing range. The longer-latency dendritic spike increases a dendrosomatic current flow to increase bursting and allows a greater segregation of information transmission by the spike train. Therefore as a result of the $GABA_B$ inhibitory feedback, isolated spikes now code preferentially for the high-frequency component of the broad band input signal (Fig. 8*E*).

Bursting in pyramidal cells

The burst dynamics of ELL pyramidal cells are well understood (Fernandez et al. 2005b; Lemon and Turner 2000; Turner et al. 1994), have been extensively modeled (Fernandez et al. 2005b; Doiron et al. 2002; Laing and Longtin 2002; Laing et

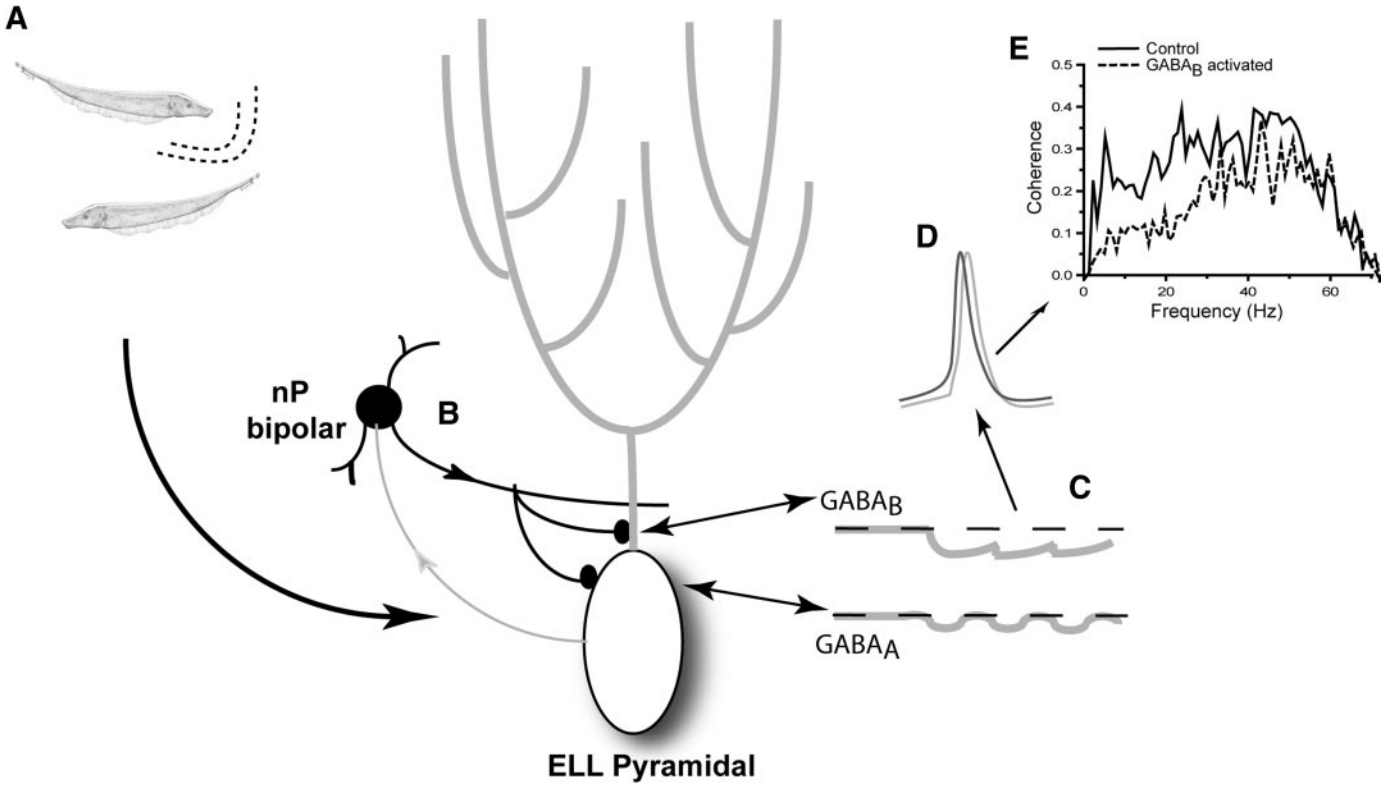

FIG. 8. Schematic of proposed mechanism to account for the shift in spike firing properties invoked by dendritic $GABA_B$ receptor activation. Spatially correlated conspecific signals (*A*) recruit the nP bipolar cell direct feedback pathway to ELL pyramidal cells (*B*). This leads to the activation of 2 synaptic currents: a $GABA_A$-mediated signal shown to drive synchronous oscillations (Doiron et al. 2003), and a more prolonged $GABA_B$ signal in the proximal dendritic and somatic region (*C*). The $GABA_B$ receptor activation leads to a decrease in burst threshold by modulating dendritic spike latency (*D*). The decrease in burst threshold increases the segregation between burst and isolated spikes by increasing the specificity of isolated spikes for high-frequency signal components so that they code entirely for conspecific signals (indicated by coherence plots in *E*).

al. 2003), and analyzed with respect to their role in sensory processing (Doiron et al. 2007; Oswald et al. 2004, 2007). Burst firing depends on an increasing delay that develops between the somatic spike and backpropagating dendritic spike during repetitive discharge (Fernandez et al. 2005b). The key variable for this delay is a cumulative dendritic sodium channel inactivation as reflected in a slowing of the rate of rise of the dendritic spike during a burst. The resulting increase in temporal separation of somatic and dendritic spikes accentuates a dendro-somatic current flow that can influence the spike generating mechanism (Fernandez et al. 2005b). Normally this process builds gradually during repetitive spike firing until the dendritic spike occurs sufficiently outside the somatic refractory period as to generate a somatic spike "doublet" that terminates the burst.

An analysis of our reduced model of burst dynamics and direct recordings from pyramidal cells suggests that $GABA_B$ inhibition is capable of delaying the dendritic spike sufficiently to bypass the gradual buildup to bursting and immediately promote spike doublets. This inhibition-induced delay of the dendritic spike required only strong hyperpolarization from synaptic currents (with $E_{rev} < -75$ mV) or from hyperpolarizing current injection in both the model and pyramidal cells. Moreover, it involved a shift in the onset latency of the dendritic spike with no effect on either spike rate of rise or amplitude. Dendritic $GABA_B$ inhibition then represents a second means by which the temporal relationship between somatic and dendritic spikes can be altered.

Bipolar cells of the nP that project in the direct feedback pathway are predicted to drive the $GABA_B$ inhibition of pyramidal cell dendrites under natural conditions. This pathway is important in that it is preferentially recruited during communication-like stimuli (Doiron et al. 2003) to activate both $GABA_A$ and $GABA_B$ receptors on pyramidal cells (Berman and Maler 1998b). Despite the inhibitory nature of this pathway, its activation in vivo leads to an increase in the number of brief ISIs (5–8 ms) that reflect intrinsic bursts in pyramidal cells (Doiron et al. 2003) (supplemental materials[1]) as well as inducing network mediated oscillatory activity (Doiron et al. 2003). It was suggested in these earlier in vivo studies that bipolar cell feedback may be responsible for increasing pyramidal cell bursts through an unknown mechanism. We find that the increase in burst activity can be accounted for when proximal dendritic $GABA_B$ inhibition compresses the tonic firing range. This is observable in the fact that in response to RAMs, the burst fraction is significantly increased during manipulations that compress the tonic firing regime. This regulation of burst dynamics is due to a shift in dendritic spike latency and causes a concomitant shift in the role of isolated spikes in encoding high-frequency inputs. This effect may be translated into an improved ability to detect both prey-like and communication signals.

We note that this process is distinct from an alternative mechanism identified in pyramidal cells in which behaviorally relevant inputs induce a network-mediated gamma oscillation that is only evoked by spatially global input arising from electrocommunication signals. The latter mechanism was shown to arise from activation of a delayed inhibitory feedback pathway from the nP that activates $GABA_A$ receptors on pyramidal cells (Doiron et al. 2003, 2004). Further studies of the feedback-induced gamma oscillation have shown that it requires fairly high-frequency input (>40 Hz) that can only be due to communication signals (B. Doiron, J. Bastian, and L. Maler, personal communication).

Work in ELL pyramidal cells thus identifies distinct roles for GABA receptor mediated inhibition activated by a descending feedback pathway in segregating spike trains for the purpose of sensory coding. It also identifies a particular role for dendritic inhibition in this process. We expect that this strategy will be active in other cells in that a decrease in the relative delay between somatic and dendritic spikes with depolarizing dendritic current has been reported (Stuart and Hausser 1994; Stuart and Sakmann 1994). $GABA_B$ inhibition was also recently shown to increase the delay between the somatic spike and backpropagating spike in hippocampus (Leung and Peloquin 2006), although potential changes in the cell's dynamics were not examined. These similarities would suggest that our results will have wide application in signifying that the mean voltage of dendritic compartments can regulate the timing of backpropagating dendritic spikes with corresponding effects on soma-dendritic interactions.

Functions of somatic and dendritic GABA receptor activation

The effects of inhibition on ELL pyramidal cell spike output are multifaceted. For instance, $GABA_A$ inhibition can cause subtractive or divisive effects on cell output depending on the location of the synapses (Mehaffey et al. 2005). Further, in the intact animal, subtractive somatic inhibition is capable of creating oscillatory activity due to feedback delays (Doiron et al. 2003). $GABA_B$-mediated inhibition targeting the basal dendrite acts as a low-pass filter to support coding for the envelope of a narrow band high-frequency signal (Middleton et al. 2006). We now show with the present results that the proximal apical dendritic $GABA_B$ receptors (but not $GABA_A$) can selectively regulate burst dynamics and in relation to activity in a specific feedback pathway. It is thus important to consider not only the type and time scale of inhibition but also the site of synaptic termination to understand the effects of inhibition on both total synaptic input and the cell's intrinsic firing dynamics.

Differential impacts of somatic and dendritic inhibition on the electrophysiological behavior of neurons have been reported previously (Mehaffey et al. 2005; Vu and Krasne 1992) and may allow different sets of inhibitory interneurons to differentially regulate patterns of spike generation. We previously described how a weaker $GABA_A$-mediated dendritic inhibition acts to reduce the gain of the F-I relationship in a divisive manner by altering dendritic spike shape (Mehaffey et al. 2005). No reduction in gain on $GABA_B$ receptor activation was observed here or in previous studies (Berman and Maler 1998b). The effects of $GABA_A$ on dendritic spikes were different, however, in that $GABA_A$ receptor activation only reduced the late phase of the dendritic spike, whereas $GABA_B$ conductances increased the relative latency of the dendritic spike. The apparent lack of effect by $GABA_B$ receptors on the late phase of the dendritic spike may simply reflect the more active components of spike discharge in proximal dendritic regions. The earlier study of Mehaffey et al. (2005) focused on

[1] The online version of this article contains supplemental data.

more distal dendritic $GABA_A$ (~100 μm) conductances that regulated the shape of the backpropagating spike. Proximal $GABA_B$ inhibition may be unable to sufficiently regulate the more narrow dendritic spike waveform inherent to more proximal regions of the dendrite, preventing the decrease in gain seen with $GABA_A$ agonists. The localization of the $GABA_B$ receptor appears to be primarily dendritic as shown by the increased hyperpolarization of dendritic membrane voltage by baclofen. The somatic membrane hyperpolarization may be due to somatic $GABA_B$ receptors or to the dendritic inhibition. Somatic $GABA_B$ receptors would be hypothesized to have a primarily subtractive effect, filtering out small-amplitude signals, but not changing the firing dynamics of the cell significantly.

One further network effect predicted by the anatomy of the ELL (Maler and Mugnaini 1994) involves the inhibition of the VML cells responsible for many of the projections that activate $GABA_A$ receptors in the proximal apical dendrites (Berman and Maler 1998a). Previous studies suggested that the nP bipolar cell provided input to VML cell somata (Maler and Mugnaini 1994). Because VML cell mediated inhibition reduces the gain of pyramidal cells (Mehaffey et al. 2005), inhibition of this interneuron should, in turn, increase the gain of pyramidal cells.

Relation of bursts to sensory coding

Sequences of patterned isolated spikes have been assumed to be the main channel for information transfer between neurons (Eggermont 1998; Rieke 1997) although the role of bursts in signal coding has begun to be studied, especially in sensory systems (Krahe and Gabbiani 2004). A segregation of spike trains into bursts and single spikes has been observed in electric fish (Gabbiani et al. 1996; Oswald et al. 2004) and in the mammalian visual (Lesica and Stanley 2004; Lesica et al. 2006) and auditory systems (Eggermont and Smith 1996). Remarkably, bursts, but not isolated spikes, predict behavior in an invertebrate preparation (Marsat and Pollack 2006). Bursts have been suggested to code for input slope (Kepecs et al. 2002) and to segregate different components of stimuli (Doiron et al. 2007; Kepecs and Lisman 2003; Oswald et al. 2007). In sensory systems, bursts have been shown to be the preferred response for low-frequency events (Lesica and Stanley 2004; Lesica et al. 2006) and specifically in the ELL for feature detection of low-frequency components of a stimulus (Doiron et al. 2007; Gabbiani et al. 1996; Metzner et al. 1998; Oswald et al. 2004, 2007). As such, burst coding appears to be an extremely common adaptation with clear benefits to information coding. When information is parceled into two distinct ranges of ISIs, the system can take advantage of differences in the postsynaptic threshold for spiking, short-term synaptic plasticity, or the intrinsic dynamics of downstream cells to separate and decode information. Such concepts have been analyzed in more detail elsewhere—in particular that bursts tend to be more reliably timed, show superior feature detection properties, and may be able to more reliably activate downstream cells than single spikes (Gabbiani et al. 1996; Izhikevich et al. 2003; Kepecs and Lisman 2003; Lisman 1997; Metzner et al. 1998).

It has recently been suggested that the slow transition in the burst dynamics (i.e., 3–5 spike/burst) is important when sensory input is comprised of low frequencies characteristic of local prey stimuli (Doiron et al. 2007). In the presence of broadband inputs consistent with both high- and low-frequency signals, pyramidal cells respond predominantly with doublets rather than full bursts (Gabbiani et al. 1996; Metzner et al. 1998; Oswald et al. 2004, 2007). Thus a compression of the tonic firing region and doublet spike discharge detected on $GABA_B$ receptor activation is consistent with the normal response to broadband inputs. The importance of the full burst dynamics for the processing of signals consisting primarily of low-frequency inputs remains to be more thoroughly examined and will require a study of the synaptic and intrinsic dynamics of midbrain target neurons (torus semicircularis, TS) (Heiligenberg 1991).

We show here that feedback-evoked synaptic currents qualitatively alter the frequency-dependent intrinsic dynamics of ELL pyramidal cells. This regulation of intrinsic pyramidal cell dynamics is predicted to occur in the specific context of communication-like signals, i.e., when these fish are foraging in groups. It has recently been shown in a related electric fish species that behaviorally induced gamma range oscillations actually improve the ability of the animal to detect prey, possibly by inducing short term depression in target cells in the TS (Ramcharitar et al. 2006). We therefore propose that when these fish forage in groups, the bipolar cell-mediated feedback inhibition has three effects that act synergistically to improve the ability of the fish to detect moving prey (low frequency) while also receiving signals from conspecifics (including high frequencies).

First the bipolar cell feedback inhibition ($GABA_A$ component) evoked by the communication signals will induce a gamma oscillation that will improve the directional selectivity of TS neurons for moving prey. Second, the same inhibitory pathway will, via its $GABA_B$ component, switch the isolated spikes into coding selectively for the high-frequency communication signals; this segregation will presumably improve the ability of TS neurons to disambiguate prey and communication signals. Third, the bipolar cell inhibition of VML cells will increase the gain of pyramidal cells, again improving their ability to code for the moving prey. Thus the complex interaction of network, synaptic and intrinsic dynamics might be required to generate a simple final result—an enhanced ability for the fish's detection of prey while foraging in groups.

ACKNOWLEDGMENTS

We thank M. Kruskic for technical assistance and B. Doiron for comments on the manuscript.

Present address of F. R. Fernandez: Neuronal Dynamics Laboratory, Department of Biomedical Engineering, Boston University, Boston, MA, 02215

GRANTS

Funding was provided by Canadian Institute of Health Research operating grants to L. Maler and R. W. Turner and CIHR studentships to W. H. Mehaffey and F. R. Fernandez and an Alberta Heritage Foundation for Medical Research studentship to W. H. Mehaffey. R. W. Turner is an AHFMR Scientist.

REFERENCES

Bastian J. Plasticity of feedback inputs in the apteronotid electrosensory system. *J Exp Biol* 202: 1327–1337, 1999.

Bastian J, Courtright J, Crawford J. Commissural neurons of the electrosensory lateral line lobe of *Apteronotus leptorhynchus:* morphological and physiological characteristics. *J Comp Physiol [A]* 173: 257–274, 1993.

Berman NJ, Maler L. Distal versus proximal inhibitory shaping of feedback excitation in the electrosensory lateral line lobe: implications for sensory filtering. *J Neurophysiol* 80: 3214–3232, 1998a.

Berman NJ, Maler L. Interaction of GABAB-mediated inhibition with voltage-gated currents of pyramidal cells: computational mechanism of a sensory searchlight. *J Neurophysiol* 80: 3197–3213, 1998b.

Berman NJ, Maler L. Inhibition evoked from primary afferents in the electrosensory lateral line lobe of the weakly electric fish (*Apteronotus leptorhynchus*). *J Neurophysiol* 80: 3173–3196, 1998c.

Berman NJ, Maler L. Neural architecture of the electrosensory lateral line lobe: adaptations for coincidence detection, a sensory searchlight and frequency-dependent adaptive filtering. *J Exp Biol* 202: 1243–1253, 1999.

Chacron MJ, Doiron B, Maler L, Longtin A, Bastian J. Non-classical receptive field mediates switch in a sensory neuron's frequency tuning. *Nature* 423: 77–81, 2003.

Cherry EC. Some experiments on the recognition of speech, with one and with two ears. *J Acous Soc Am* 25: 975–979, 1953.

Doedel EJ. AUTO: a program for the automatic bifurcation analysis of autonomous systems. In: *Congressus Numerantium.* Winnipeg, Canada: Utilitas Mathematica Publishing, 1981, p. 265–284.

Doiron B, Chacron MJ, Maler L, Longtin A, Bastian J. Inhibitory feedback required for network oscillatory responses to communication but not prey stimuli. *Nature* 421: 539–543, 2003.

Doiron B, Laing C, Longtin A, Maler L. Ghostbursting: a novel neuronal burst mechanism. *J Comput Neurosci* 12: 5–25, 2002.

Doiron B, Lindner B, Longtin A, Maler L, Bastian J. Oscillatory activity in electrosensory neurons increases with the spatial correlation of the stochastic input stimulus. *Phys Rev Lett* 93: 048101, 2004.

Doiron B, Oswald AM, Maler L. Interval coding. II. Dendrite-dependent mechanisms. *J Neurophysiol* 97: 2744–2757, 2007.

Eggermont JJ. Is there a neural code? *Neurosci Biobehav Rev* 22: 355–370, 1998.

Eggermont JJ, Smith GM. Burst-firing sharpens frequency-tuning in primary auditory cortex. *Neuroreport* 7: 753–757, 1996.

Ermentrout B. *Simulating, Analyzing, and Animating Dynamical Systems: A Guide to XPPAUT for Researchers and Students.* Philadelphia: Society for Industrial and Applied Mathematics, 2002

Fahle M. Figure-ground discrimination from temporal information. *Proc Biol Sci* 254: 199–203, 1993.

Fernandez FR, Mehaffey WH, Molineux ML, Turner RW. High-threshold K^+ current increases gain by offsetting a frequency-dependent increase in low-threshold K^+ current. *J Neurosci* 25: 363–371, 2005a.

Fernandez FR, Mehaffey WH, Turner RW. Dendritic Na^+ current inactivation can increase cell excitability by delaying a somatic depolarizing afterpotential. *J Neurophysiol* 94: 3836–3848, 2005b.

Fritz JB, Elhilali M, David SV, Shamma SA. Does attention play a role in dynamic receptive field adaptation to changing acoustic salience in A1? *Hear Res* 29: 186–203, 2007.

Gabbiani F, Metzner W, Wessel R, Koch C. From stimulus encoding to feature extraction in weakly electric fish. *Nature* 384: 564–567, 1996.

Haykin S, Chen Z. The cocktail party problem. *Neural Comput* 17: 1875–1902, 2005.

Heiligenberg W. *Neural Nets in Electric Fish.* Cambridge, MA: MIT Press, 1991.

Izhikevich EM, Desai NS, Walcott EC, Hoppensteadt FC. Bursts as a unit of neural information: selective communication via resonance. *Trends Neurosci* 26: 161–167, 2003.

Kepecs A, Lisman J. Information encoding and computation with spikes and bursts. *Network* 14: 103–118, 2003.

Kepecs A, Wang XJ, Lisman J. Bursting neurons signal input slope. *J Neurosci* 22: 9053–9062, 2002.

Krahe R, Gabbiani F. Burst firing in sensory systems. *Nat Rev Neurosci* 5: 13–23, 2004.

Laing CR, Longtin A. A two-variable model of somatic-dendritic interactions in a bursting neuron. *Bull Math Biol* 64: 829–860, 2002.

Laing CR, Doiron B, Longtin A, Noonan L, Turner RW, Maler L. Type I burst excitability. *J Comput Neurosci* 14: 329–342, 2003.

Lemon N, Turner RW. Conditional spike backpropagation generates burst discharge in a sensory neuron. *J Neurophysiol* 84: 1519–1530, 2000.

Lesica NA, Stanley GB. Encoding of natural scene movies by tonic and burst spikes in the lateral geniculate nucleus. *J Neurosci* 24: 10731–10740, 2004.

Lesica NA, Weng C, Jin J, Yeh CI, Alonso JM, Stanley GB. Dynamic encoding of natural luminance sequences by LGN bursts. *PLoS Biol* 4: e209, 2006.

Leung LS, Peloquin P. GABA(B) receptors inhibit backpropagating dendritic spikes in hippocampal CA1 pyramidal cells in vivo. *Hippocampus* 16: 388–407, 2006.

Lindner B, Doiron B, Longtin A. Theory of oscillatory firing induced by spatially correlated noise and delayed inhibitory feedback. *Phys Rev E Stat Nonlin Soft Matter Phys* 72: 061919, 2005.

Lisman JE. Bursts as a unit of neural information: making unreliable synapses reliable. *Trends Neurosci* 20: 38–43, 1997.

MacIver MA, Sharabash NM, Nelson ME. Prey-capture behavior in gymnotid electric fish: motion analysis and effects of water conductivity. *J Exp Biol* 204: 543–557, 2001.

Mainen ZF, Sejnowski TJ. Influence of dendritic structure on firing pattern in model neocortical neurons. *Nature* 382: 363–366, 1996.

Maler L, Mugnaini E. Correlating gamma-aminobutyric acidergic circuits and sensory function in the electrosensory lateral line lobe of a gymnotiform fish. *J Comp Neurol* 345: 224–252, 1994.

Maler L, Sas E, Johnston S, Ellis W. An atlas of the brain of the electric fish *Apteronotus leptorhynchus. J Chem Neuroanat* 4: 1–38, 1991.

Marsat G, Pollack GS. A behavioral role for feature detection by sensory bursts. *J Neurosci* 26: 10542–10547, 2006.

Mehaffey WH, Doiron B, Maler L, Turner RW. Deterministic multiplicative gain control with active dendrites. *J Neurosci* 25: 9968–9977, 2005.

Metzner W, Koch C, Wessel R, Gabbiani F. Feature extraction by burst-like spike patterns in multiple sensory maps. *J Neurosci* 18: 2283–2300, 1998.

Middleton JW, Longtin A, Benda J, Maler L. The cellular basis for parallel neural transmission of a high-frequency stimulus and its low-frequency envelope. *Proc Natl Acad Sci USA* 103: 14596–14601, 2006.

Noonan L, Doiron B, Laing C, Longtin A, Turner RW. A dynamic dendritic refractory period regulates burst discharge in the electrosensory lobe of weakly electric fish. *J Neurosci* 23: 1524–1534, 2003.

Oswald AM, Chacron MJ, Doiron B, Bastian J, Maler L. Parallel processing of sensory input by bursts and isolated spikes. *J Neurosci* 24: 4351–4362, 2004.

Oswald AM, Doiron B, Maler L. Interval coding. I. Burst interspike intervals as indicators of stimulus intensity. *J Neurophysiol* 97: 2731–2743, 2007.

Pinsky PF, Rinzel J. Intrinsic and network rhythmogenesis in a reduced Traub model for CA3 neurons. *J Comput Neurosci* 1: 39–60, 1994.

Ramcharitar JU, Tan EW, Fortune ES. Global electrosensory oscillations enhance directional responses of midbrain neurons in *Eigenmannia. J Neurophysiol* 96: 2319–2326, 2006.

Rieke F. *Spikes: Exploring the Neural Code.* Cambridge, MA: MIT Press, 1997.

Rinzel J, Ermentrout B. Analysis of neural excitability and oscillations. In: *Methods in Neuronal Modelling: From Synapses to Networks* (2nd ed.), edited by Koch C, Segev I. Cambridge, MA: MIT Press, 1998, p. 251–291.

Stuart G, Hausser M. Initiation and spread of sodium action potentials in cerebellar Purkinje cells. *Neuron* 13: 703–712, 1994.

Stuart GJ, Sakmann B. Active propagation of somatic action potentials into neocortical pyramidal cell dendrites. *Nature* 367: 69–72, 1994.

Tan EW, Nizar JM, Carrera GE, Fortune ES. Electrosensory interference in naturally occurring aggregates of a species of weakly electric fish, *Eigenmannia virescens. Behav Brain Res* 164: 83–92, 2005.

Turner RW, Maler L, Deerinck T, Levinson SR, Ellisman MH. TTX-sensitive dendritic sodium channels underlie oscillatory discharge in a vertebrate sensory neuron. *J Neurosci* 14: 6453–6471, 1994.

Turner RW, Meyers DE, Richardson TL, Barker JL. The site for initiation of action potential discharge over the somatodendritic axis of rat hippocampal CA1 pyramidal neurons. *J Neurosci* 11: 2270–2280, 1991.

Ulrich D. Differential arithmetic of shunting inhibition for voltage and spike rate in neocortical pyramidal cells. *Eur J Neurosci* 18: 2159–2165, 2003.

Vu ET, Krasne FB. Evidence for a computational distinction between proximal and distal neuronal inhibition. *Science* 255: 1710–1712, 1992.

Wang XJ. Fast burst firing and short-term synaptic plasticity: a model of neocortical chattering neurons. *Neuroscience* 89: 347–362, 1999.

Zupanc GK, Sirbulescu RF, Nichols A, Ilies I. Electric interactions through chirping behavior in the weakly electric fish, *Apteronotus leptorhynchus. J Comp Physiol [A]* 192: 159–173, 2006.